BOLETIN DE LA SOCIEDAD ESPAÑOLA DE
Cerámica y Vidrio
www.elsevier.es/bsecv

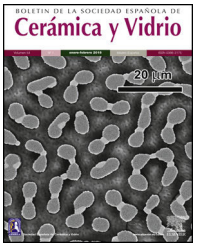

Structural properties, linear, and non-linear optical parameters of ternary $Se_{80}Te_{(20-x)}In_x$ chalcogenide glass systems

Saeid M. Elkatlawy[a,*], *Ahmed H. El-Dosokey*[b], *Hossam M. Gomaa*[c]

[a] *Department of Physics, Faculty of Science, Damanhour University, 22111 Damanhour, Egypt*
[b] *Department of Physics, Faculty of Science, El-Fayoum University, El-Fayoum, Egypt*
[c] *Independent Researcher, Sakkara, Giza, Egypt*

ARTICLE INFO

Article history:
Received 17 July 2020
Accepted 22 September 2020
Available online 21 October 2020

Keywords:
Chalcogenide glasses
Thin films
Linear optical parameters
Nonlinear optical parameters
IR waveguides
IR sensors

ABSTRACT

Ternary chalcogenide glass systems of $Se_{80}Te_{(20-x)}In_x$, where $x = 0$, 5, 10 wt.%, were synthesized via fast quenching of their melts. Bulk samples were ground into fine powder and thermally evaporated onto silica glass substrate, under vacuum, in order to obtain homogeneous thin films. DSC analysis of bulk samples revealed the presence of small endothermic peak, that identifies the glass transition temperature T_g, followed by an exothermic peak that defines the amorphous-crystalline phase transition T_p. These results confirmed the amorphous nature of the bulk samples. XRD analysis confirmed the amorphous nature of the studied thin films. Inclusion of indium in the glass matrix contributed to elevating refractive index and showed wide transmission window in the visible and near IR regions. Linear and nonlinear optical parameters are calculated and discussed in terms of the glass composition. Results of refractive index, first and third order susceptibilities nominate the studied thin films for applications in IR waveguides and sensors.

Análisis estructural y parámetros ópticos lineales y no lineales de sistemas ternarios de vidrio de calcogenuro de composición $Se_{80}Te_{(20-x)}In_x$

Palabras clave:
Vidrio de calcogenuro
Películas delgadas
Parámetros ópticos lineales y no lineales
Guías ópticas y sensores de ondas IR

RESUMEN

Los sistemas ternarios de vidrio de calcogenuro de composición $Se_{80}Te_{(20-x)}In_x$, en los que x = 0, 5, 10 wt.%, se prepararon mediante enfriamiento rápido de sus fundidos. Las muestras a granel se molieron en polvo fino y se evaporaron térmicamente sobre sustrato de vidrio de sílice, en el vacío, para obtener películas delgadas homogéneas. El análisis DSC de muestras a granel reveló la presencia de un pequeño pico endotérmico que identifica la temperatura de transición vítrea T_g, seguido de un pico exotérmico que define la transición de fase cristalina-amorfa T_p. Estos resultados confirmaron la naturaleza amorfa de las

* *Corresponding author.*
E-mail address: elkatlawy@sci.dmu.edu.eg (S.M. Elkatlawy).
https://doi.org/10.1016/j.bsecv.2020.09.007

muestras a granel. El análisis XRD confirmó la naturaleza amorfa de las películas delgadas estudiadas. La inclusión de indio en la matriz de vidrio contribuyó a elevar el índice de refracción y mostró una amplia ventana de transmisión en las regiones de espectro visible e IR-cercano. Los parámetros ópticos lineales y no lineales se calculan y analizan en términos de la composición del vidrio. Los resultados del índice de refracción, las susceptibilidades de primer y tercer orden nominan las películas delgadas estudiadas para aplicaciones en guías ópticas y sensores de ondas IR.

Introduction

Thin films deposited from chalcogenide glasses have several potential applications in optical communications, opto-electronic applications, and solar cells [1]. Chalcogenide glasses are based mainly on chalcogen elements Sulfur, Selenium, and Tellurium and are formed by bonding to network forming elements of comparable electronegativity, such as In, Sn, Si, Ge, Ga and Cd [2–5]. On the other hand, infrared glasses are mainly based on covalently bonded elements of comparable values of electronegativity. In this regard, chalcogenide glasses are covalently bonded, possess a weak inter-atomic bonding, and they look more like polymers. They show much interest in diverse areas of applications because of their transparency in the near- and mid- IR spectral regions, high refractive index, and excellent non-linear behavior [6,7]. Due to these structural characteristics, chalcogenide glasses are ideal for infrared and nonlinear optics, bio-sensors, and waveguide applications [7,8]. Chalcogenide glasses have shown fast response to optical non-linearity over conventional silicon-based glasses [9]. On the other hand, synthesis process and the glass compositional ratios can strongly govern the desired properties of the obtained chalcogenide based thin films [10]. Selenium and tellurium based glasses are having notable glass-forming ability and good integration with other elements with comparable electronegativity [4,11]. In this regard, ternary glass systems make it possible for more atoms to incorporate into the glass matrix resulting in improved properties. Se–Te system is most studied due to its functionality as glass host matrix and its elevated glass forming ability. However, physical properties of these glasses were reported to be improved by dopant elements [12,13]. Incorporating metallic elements to the Se–Te glass matrix resulted in high thermal stability of the system [14,15]. Additionally, metallic dopants were reported to improve chalcogenide glass characteristics such as optical, electrical, and mechanical properties [5]. Indium doping was reported to expand the glass forming region and increase the disorder in the system which leads to wider areas of applications [7,16]. On the other hand, chalcogenide glasses were reported to possess elevated values of the nonlinear optical parameters [17]. It was also reported that materials with elevated optical nonlinearity have potential applications in photonics, optoelectronics, and optical sensing applications [18].

In the present study, the effect of partial replacement of tellurium by indium on structural, physical, and optical properties of Se–Te–In chalcogenide thin films is studied. Linear and non-linear optical parameters are calculated and discussed in terms of glass composition.

Experimental details

Three chalcogenide glass' matrices containing different concentrations (in wt.%) of Se, Te, and In elements were prepared, from high purity chemicals (99.999%), using the melt quench technique. The following chemical formula describes the ratio of each constituent in the ternary glass system: $80\,\text{wt.\%}\,\text{Se} \cdot (20 - x)\,\text{wt.\%}\,\text{Te} \cdot x\,\text{wt.\%}\,\text{In}$, where, $x = 0$, 5, and 10 wt.%. Where suitable amount of raw elements (calculated according to atomic weight and constituent ratio) were introduced and sealed in evacuated silica tubes (at pressure of $\sim 10^{-5}$ Torr) in order to avoid sample oxidation. Samples were then heated at $800 \pm 5\,^{\circ}\text{C}$ in horizontal furnace for up to 15 h. Prior to heating, tubes were treated in an ultrasonic cleaner and cleaned several times using detergent and double distilled water, and a final washing with ethyl alcohol. Continuous rocking of the tubes during heating was necessary in order to maintain homogeneity and uniformity of the melts. Finally, the molten materials were quenched into iced water to avoid any sort of crystallization.

The obtained bulk glass' samples were ground into powder using hydraulic pressing under vacuum, in order to be used to prepare thin films. A suitable amount of the powdered material was positioned into a Molybdenum Boat and evaporated on a silica glass (SG) substrate under high vacuum of $\sim 2 \times 10^{-5}$ Torr using a standard Edwards A306 Auto coating unit with conventional rotary and turbo molecular pumps. Prior to use, SG substrates were cleaned several times before being mounted in the rotating substrate work holder, with adjusted rotating speed that allows the production of highly homogeneous films.

Differential scanning calorimetry was employed to perform thermal analysis of the studied bulk samples, using a DSC6220 calorimeter from EXSTAR SII with accuracy of 0.1 K. Samples were scanned at different heating rates, using a 3 mg sample amount, in the temperature range from 300 to 580 K. Before each heating cycle, calorimeter was calibrated using the well-known melting enthalpy of indium. Amorphous nature of thin film samples was confirmed via XRD using Shimadzu XRD-7000 diffractometer, with a Cu Kα radiation of $\lambda = 1.5406$ Å, at scan rate of 2°/min, in the 2θ range from 10° to 90°. Optical analysis was performed using an Evolution 600 UV-Vis spectrophotometer from Thermo scientific USA, in the spectrum range from 190 to 1100 nm.

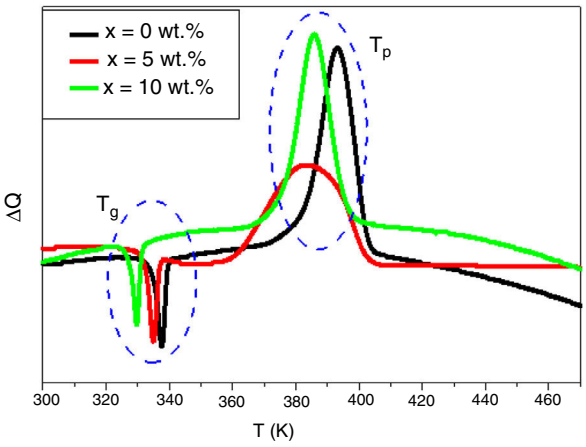

Fig. 1 – DSC thermograms at fixed heating rate (5 K/min) for the three bulk glass samples with different In content.

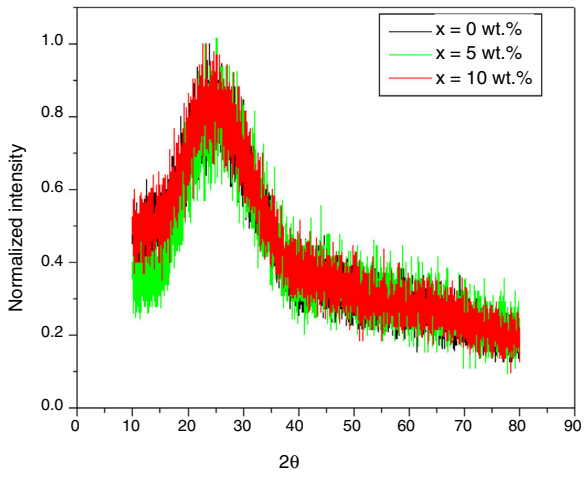

Fig. 2 – Normalized XRD for x = 0, 5 and 10 wt.% thin film samples.

Table 1 – DSC parameters.

x (wt.%)	T_g (K)	T_p (K)	$T_p - T_g$
0	337	393	56
5	334	388	54
10	329	385	56

Results and discussion

Thermal analysis

DSC thermograms of the three studied bulk samples, at fixed heating rate ($\beta = 5$ K/min) are shown in Fig. 1. It can be observed that each thermogram exhibits small endothermic peak followed by an exothermic peak. The endothermic peak identifies the amorphous solids and is used to determine the glass transition temperature T_g, while the exothermic peak refers to the crystallization temperature T_p. Values of both T_g and T_p, for all studied samples, were determined and tabulated in Table 1. Fig. 1 manifests that each sample possess only one glass transition temperature and only one crystallization temperature, which indicate the highly homogenous amorphous glass. These results agree with similar systems published in the literature [15,19,20]. Checking data in Table 1 shows the glass transition point shifted to the lower temperatures as the amount of In was increased from 0 wt.% to 10 wt.%. That is to say, the partial replacement of tellurium by indium perturbs the thermal stability of $Se_{80}Te_{20-x}In_x$ chalcogenide glasses. Referring to the literature, the position of T_g point depends on several factors such as bond energy, molecular weight, and the coordination number [21,22]. Replacing Te by In in the present glass system contributed to lowering the position of T_g point, in agreement with published literature [14,23]. This is due to the decrease in the amount of tellurium in the glass matrix [20]. From Table 1 the difference between T_p and T_g values is calculated, for each sample, and depending on this difference one can state that the sample of x = 5 wt.% showed low glass forming ability. This action might be attributed to an experimental error during preparation process, possibly a long cooling rate.

XRD analysis

The value of the optical band gap of the studied materials was reported to depend on the existance of short-range order [24]. In this regard, XRD analysis gives an insightful confirmation on the amorphous nature of the glass thin films. Fig. 2 shows normalized XRD diffractograms for the thin films. It is clear that all diffractograms are nearly identical which means that all samples interact with X-rays by the same mechanism. The appearance of only semi-broad hump, for each sample, with no sharp peaks, confirms the amorphous nature of the thin films.

Linear optical parameters of thin films

Fig. 3 manifests the variations of the values for both absorbance (A%) and transmittance (T%) of the studied films, respectively, vs. wavelength in nm. Both A% and T% values were affected by increasing the value of x, especially in the wavelength ranged between 450 and ~700 nm, where A% values increased while T% decreased when x value was increased. Refractive index is directly related to optical density of the material, more optically dense materials have higher refractive indices. In this regard, the strong absorption is related to the more optically dense medium and, subsequently, an increase in the value of the refractive index [25]. In the present work, indium incorporation contributed to increasing the optical density of the material, due to the metallic nature of indium, and consequently, increased the value of refractive index. This high refractive index together with structural properties of the glass, may nominate the studied films for infrared waveguides and sensor applications [7,8].

Depending on both T% and A%, the absorption coefficient α was calculated for all studied films, as seen in Fig. 4. The optical absorption coefficient is a good parameter that yields useful information about how far light of a particular wavelength can penetrate into a particular matter-phase before it is absorbed. In this regard, materials with high transparency have low absorption coefficients, and vice versa [26].

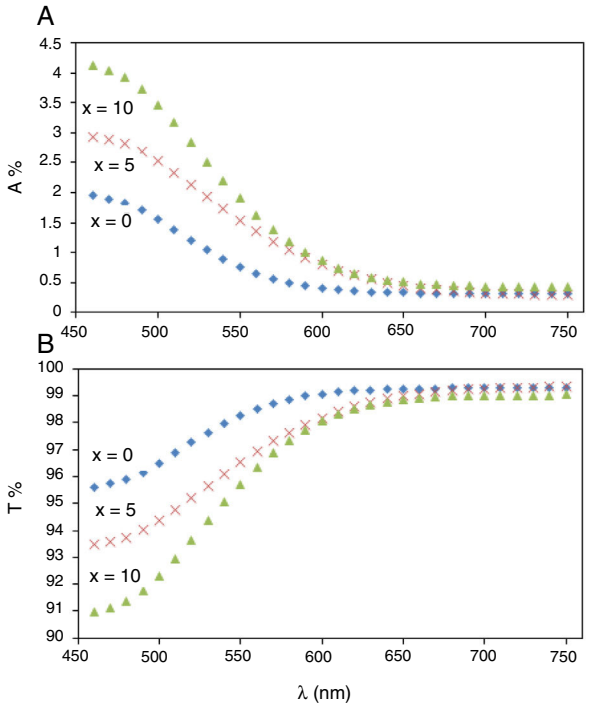

Fig. 3 – Absorbance A% (A) and transmittance T% (B) vs. wavelength for as deposited thin film samples, with different amounts of In (0, 5, 10 wt.%).

The optical absorption coefficient α depends on the thickness of the material and the energy of the incident photons, as shown by the following relationships [27,28]:

$$\alpha = \frac{A}{t}(cm^{-1}) \quad (1)$$

$$\alpha = \alpha_o e^{E_{ph}/E_u} \quad (2)$$

where A is the optical absorption, t is sample's thickness, E_{ph} is the incident photon energy, E_U is Urbach energy or Urbach tails absorption which is useful mechanism to describe the absorption processes when $10 < \alpha < 10^4\ cm^{-1}$ [18]. Fig. 4A shows that the indium-free sample has low absorption coefficient and is the most transparent. Also, it's clear that the transparency decreases with increasing amount of In from 0 wt.% to 10 wt.%. Such observation leads to the conclusion that the optical band gap of the studied films is reduced when partially replacing Te by In. This result agrees with published work [29]. This is due to the metallic nature of In and also might be due to the fact the In has lower ionization energy (5.7864 eV) than Te (9.0096 eV). Fig. 4B shows the relationship between Ln (α) and the energy of incident photons ($h\nu$). Using Fig. 4B, values for α_o (intersect point of the straight lines) and E_U (inverse of the slope of tangent) were obtained then recorded in Table 2. As manifested in Table 2, the Urbach Energy values are too small and are decreasing with increasing the In amount (value for x), which may indicates high homogeneous disorder phase in the studied films.

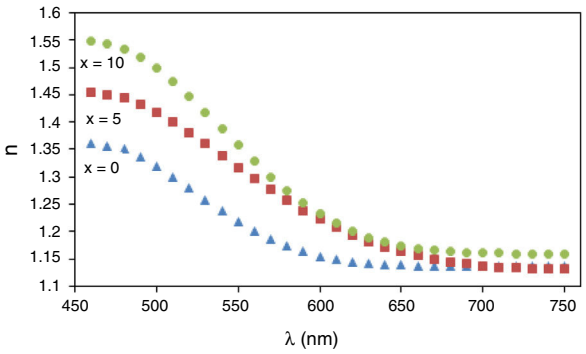

Fig. 5 – Charts of linear refractive index for x = 0, 5 and 10 wt.%.

On the other hand, linear parameters were calculated, and linear refractive index vs. wavelength is shown in Fig. 5. The value of the linear refractive index decreased for each sample with increasing the photon wavelength. Additionally, as predicted in the previous section, the value of the refractive index increased with increasing the x value, such behavior may refer to an increase in the atomic packing density as a result of replacing Te – element of relatively high atomic (Van der Waals) radius (206 pm) – by In – element of relatively low atomic radius (193 pm).

Wemple–DiDomenico Single Effective Oscillator model [30] is used to correlate the linear refractive index to the single

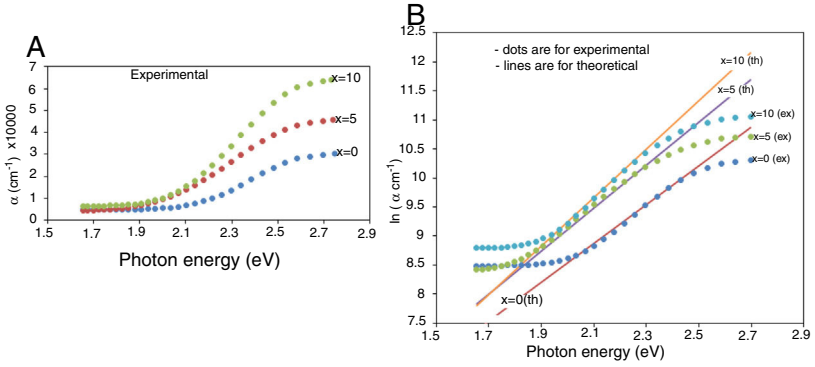

Fig. 4 – Absorption coefficient (α) (A), Ln (α) (B) vs. the photon energy (eV) for as deposited thin film samples, with different amounts of In (0, 5, 10 wt.%).

Table 2 – Linear optical parameters for as deposited films.

x (wt.%)	α_o (cm^{-1})	E_U (eV)	E_o/E_d	$1/E_oE_d$	E_o (eV)	E_d (eV)	E_g (eV)	n_o
0	6.5	0.30	2.67	-4.04	0.81	0.30	0.41	1.37
5	5.5	0.27	2.46	-4.06	0.78	0.32	0.39	1.40
10	2.5	0.24	2.43	-4.01	0.78	0.32	0.39	1.41

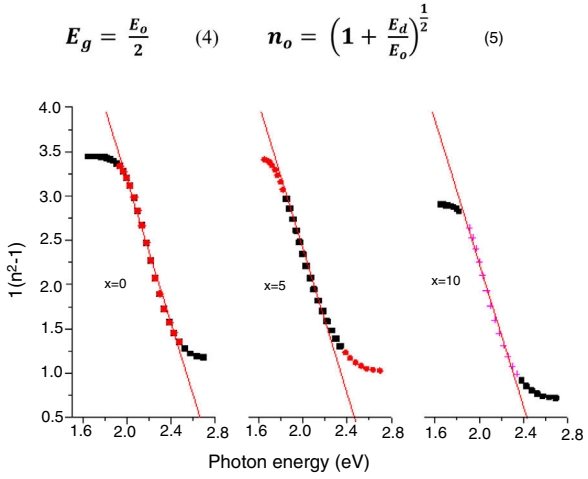

Fig. 6 – $1/(n^2-1)$ versus the photon energy for x = 0, 5 and 10 wt.%.

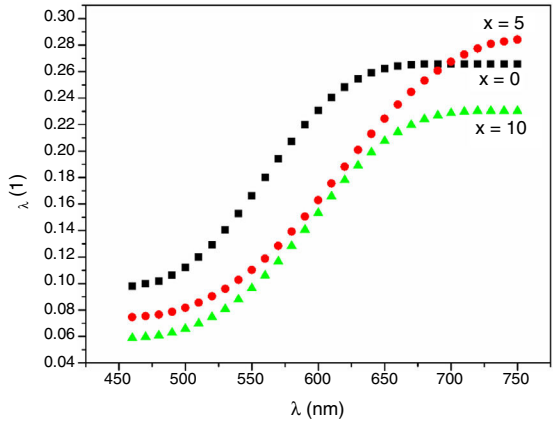

Fig. 7 – First order optical susceptibility vs. photon wavelength for all samples.

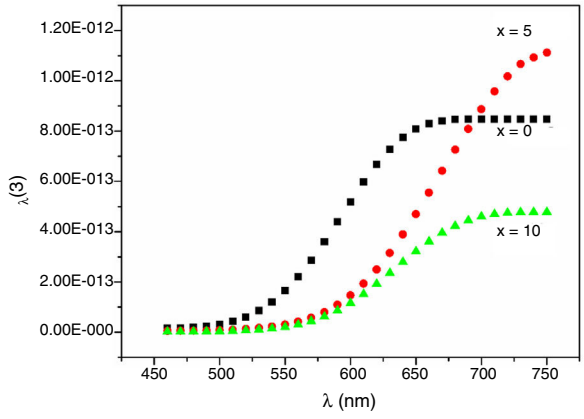

Fig. 8 – Third order optical susceptibility vs. photon wavelength for all samples.

oscillator energy E_o and dispersion energy E_d by the following relation (3).

$$\frac{1}{n^2-1} = \frac{E_o}{E_d} - \frac{E_{photon}}{E_oE_d} \quad (3)$$

E_o and E_d can be obtained by plotting $1/n^2-1$ versus E_{Photon} which is a curve. The slope of the curve's straight section represents $1/E_oE_d$, while its intersect with the abscissa represent E_o/E_d, as seen in Fig. 6. Both E_o and E_d are useful to obtain the optical band gap E_g and the static refractive index n_o for the studied films according to relations (4) and (5) [18], as listed in Table 2.

$$E_g = \frac{E_o}{2} \quad (4)$$

$$n_o = \left(1 + \frac{E_d}{E_o}\right)^{1/2} \quad (5)$$

Non-linear optical parameters of thin films

Nonlinear optical parameters, namely, first order optical susceptibility $\chi^{(1)}$, third order optical susceptibility $\chi^{(3)}$, and nonlinear refractive index $n^*(\lambda)$ are very important when studying the interaction of high-intensity light with mater. In this concern, these parameters can be calculated in terms of the linear refractive index using the following relations (6)–(8) [17,18].

$$X^{(1)} = \frac{n^2-1}{4\pi} \quad (6)$$

$$X^{(3)} = \frac{1.7 * 10^{-10}}{(4\pi)^4}\left[n^2-1\right]^4 \quad (7)$$

$$n^*(\lambda) = \frac{12\pi X^{(3)}}{n(\lambda)} \quad (8)$$

Figs. 7 and 8 show the photon-wavelength dependence of both first order and third order susceptibilities, respectively. For the studied films, both susceptibilities showed gradual increase with increasing wavelength of the incident photon, up to saturation point, which shifted to the higher wavelength as In amount was increased. Such observation may be due to the difference in the ionization energies of both Te and In. Also, it is clearly seen that for fixed wavelength, the values of both susceptibilities decreased with exchanging Te by In, but the midpoint sample (x = 5) has a nominal behavior around

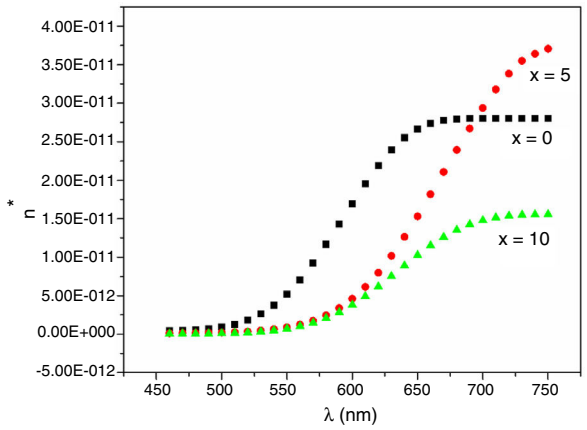

Fig. 9 – Nonlinear refractive index vs. photon wavelength for all samples.

675 nm. Such sample showed to possess, at his point, higher susceptibilities' values. Authors have not any explanation for such observation, but they decide to report it for readers. Generally, the increase in susceptibilities' values with increasing the photon wavelength may refer to an increase in the probability of photon-film interaction with replacement of Te by In.

Fig. 9 depicts the variation of the nonlinear refractive index as a function of the incident photon wavelength, where it shows identical behavior to that of the third order susceptibilities. In other word, for the studied films, the nonlinear refractive index depends of the third order susceptibility.

Conclusions

In this work, three chalcogenide glasses of the composition $Se_{80}Te_{(20-x)}In_x$, where $x = 0$, 5, 10, were synthesized via fast quenching of their melts. Bulk samples were studied by differential scanning calorimetry in order to check for their internal nature. Results showed that bulk samples possess only small endothermic peak for each sample, that identifies the glass transition temperature T_g, followed by an exothermic peak that defines the amorphous-crystalline phase transition T_p. Values for T_g and T_p were decreased when increasing the amount of In. These results confirmed the amorphous nature of the bulk samples. On the other hand, powdered bulk samples were thermally evaporated to prepare three planner thin films of the glass composition. XRD analysis confirmed the amorphous nature of the studied thin films. Optical absorbance and transmittance were recorded and used to calculate absorption coefficient, refractive index, and band gap. Indium incorporation to the glass matrix contributed to elevating refractive index and showed wide transmission window in the visible and near IR regions. Nonlinear optical parameters were calculated using values of refractive index and discussed in terms of the glass composition. Results of nonlinear refractive index, first and third order optical susceptibilities nominate the studied thin films for applications in IR waveguides and optical sensors.

REFERENCES

[1] A.S. Hassanien, A.A. Akl, Effect of Se addition on optical and electrical properties of chalcogenide CdSSe thin films, Superlattices Microstruct. 89 (2016) 153–169, http://dx.doi.org/10.1016/j.spmi.2015.10.044.
[2] T. Wang, O. Gulbiten, R. Wang, Z. Yang, A. Smith, B. Luther-Davies, P. Lucas, Relative contribution of stoichiometry and mean coordination to the fragility of Ge–As–Se glass forming liquids, J. Phys. Chem. B 118 (2014) 1436–1442, http://dx.doi.org/10.1021/jp412226w.
[3] S. Kumar, Nirjhar, A. Sakshi, Singh, Study of glass-forming ability and structural rigidity of Zn-modified $(GeTe)_x(Sb_2Te_3)100_{-x}$ chalcogenide glassy alloys, Phase Trans. 93 (2020) 183–196, http://dx.doi.org/10.1080/01411594.2019.1679367.
[4] A. Zakery, S. Elliott, Optical properties and applications of chalcogenide glasses: a review, J. Non. Cryst. Solids 330 (2003) 1–12, http://dx.doi.org/10.1016/j.jnoncrysol.2003.08.064.
[5] I. Sharma, P. Kumar, S. Tripathi, Physical and optical properties of bulk and thin films of a–Ge–Sb–Te lone-pair semiconductors, Phase Trans. 90 (2017) 653–671, http://dx.doi.org/10.1080/01411594.2016.1260720.
[6] P.K. Singh, D.K. Dwivedi, Chalcogenide glass: fabrication techniques, properties and applications, Ferroelectrics 520 (2017) 256–273, http://dx.doi.org/10.1080/00150193.2017.1412187.
[7] A. Zakery, S. Elliott, Optical Nonlinearities in Chalcogenide Glasses and their Applications, Springer Berlin Heidelberg, Berlin Heidelberg, 2007, http://dx.doi.org/10.1007/978-3-540-71068-4.
[8] B.J. Eggleton, B. Luther-Davies, K. Richardson, Chalcogenide photonics, Nat. Photonics 5 (2011) 141–148, http://dx.doi.org/10.1038/nphoton.2011.309.
[9] J.W. Choi, Z. Han, B.-U. Sohn, G.F.R. Chen, C. Smith, L.C. Kimerling, K.A. Richardson, A.M. Agarwal, D.T.H. Tan, Nonlinear characterization of GeSbS chalcogenide glass waveguides, Sci. Rep. 6 (2016), http://dx.doi.org/10.1038/srep39234.
[10] M. Frumar, B. Frumarova, T. Wagner, Amorphous and glassy semiconducting chalcogenides, in: Compr. Semicond. Sci. Technol., Elsevier, 2011, pp. 206–261, http://dx.doi.org/10.1016/B978-0-44-453153-7.00122-X.
[11] J. Sanghera, I. Aggarwal, Active and passive chalcogenide glass optical fibers for IR applications: a review, J. Non. Cryst. Solids 256–257 (1999) 6–16, http://dx.doi.org/10.1016/S0022-3093(99)00484-6.
[12] A.S. Hassanien, I. Sharma, Optical properties of quaternary a-$Ge_{15-x}Sb_xSe_{50}Te_{35}$ thermally evaporated thin-films: refractive index dispersion and single oscillator parameters, Optik (Stuttg.) 200 (2020) 163415, http://dx.doi.org/10.1016/j.ijleo.2019.163415.
[13] J. Lucas, J. Troles, X.H. Zhang, C. Boussard-Pledel, M. Poulain, B. Bureau, Glasses to see beyond visible, Comptes Rendus Chim. 21 (2018) 916–922, http://dx.doi.org/10.1016/j.crci.2018.02.010.
[14] K.A. Aly, F.M. Abdel Rahim, A. Dahshan, Thermal analysis and physical properties of Bi–Se–Te chalcogenide glasses, J. Alloys Compd. 593 (2014) 283–289, http://dx.doi.org/10.1016/j.jallcom.2014.01.057.
[15] M.M. Soraya, E.R. Shaaban, M.A. Awad, H.S. Hassan, M.I. Eman, H. Algarni, Effect of replacement of selenium by indium on the thermal stability and crystallization kinetics of quaternary Se_{90-x}–Zn_5–Te_5–In_x glassy alloys, Appl. Phys. A 124 (2018) 197, http://dx.doi.org/10.1007/s00339-018-1603-8.
[16] K. Wang, C. Steimer, D. Wamwangi, S. Ziegler, M. Wuttig, Effect of indium doping on $Ge_2Sb_2Te_5$ thin films for

phase-change optical storage, Appl. Phys. A 80 (2005) 1611–1616, http://dx.doi.org/10.1007/s00339-005-3232-2.
[17] J.S. Sanghera, C.M. Florea, L.B. Shaw, P. Pureza, V.Q. Nguyen, M. Bashkansky, Z. Dutton, I.D. Aggarwal, Non-linear properties of chalcogenide glasses and fibers, J. Non. Cryst. Solids 354 (2008) 462–467, http://dx.doi.org/10.1016/j.jnoncrysol.2007.06.104.
[18] H.M. Gomaa, I.S. Ali, A.S. Morsy, M.I. Sayyed, Linear/nonlinear optical parameters of niobium-free and niobium-doped bismuth borate glass samples, Appl. Phys. A 126 (2020) 384, http://dx.doi.org/10.1007/s00339-020-03552-z.
[19] R. Ansari, H. Kumar, Calorimetric study of crystallization kinetics in ternary alloys of Se–Te–Sn glasses using iso-conversional approach, Boletín La Soc. Española Cerámica y Vidr. (2020), http://dx.doi.org/10.1016/j.bsecv.2020.01.002.
[20] R. Svoboda, J. Málek, Thermal behavior in Se–Te chalcogenide system: interplay of thermodynamics and kinetics, J. Chem. Phys. 141 (2014) 224507, http://dx.doi.org/10.1063/1.4903543.
[21] M.K. Rabinal, K.S. Sangunni, E.S.R. Gopal, Chemical ordering in $Ge_{20}Se_{80-x}In_x$ glasses, J. Non. Cryst. Solids 188 (1995) 98–106, http://dx.doi.org/10.1016/0022-3093(94)00699-7.
[22] A. Giridhar, S. Mahadevan, The Tg versus Z dependence of glasses of the Ge–In–Se system, J. Non. Cryst. Solids 151 (1992) 245–252, http://dx.doi.org/10.1016/0022-3093(92)90036-J.
[23] G. Abbady, A.M. Abd-Elnaiem, Thermal stability and crystallization kinetics of $Ge_{13}In_8Se_{79}$ chalcogenide glass, Phase Trans. 92 (2019) 667–682, http://dx.doi.org/10.1080/01411594.2019.1619178.
[24] A.R. Ioffe, A.F. Regel, Non-crystalline, amorphous, and liquid electronic semiconductors, in: Prog. Semicond., John Wiley, New York, NY, 1960: pp. 237–291.
[25] N.M. Ravindra, P. Ganapathy, J. Choi, Energy gap–refractive index relations in semiconductors – an overview, Infrared Phys. Technol. 50 (2007) 21–29, http://dx.doi.org/10.1016/j.infrared.2006.04.001.
[26] R. Naik, J. Pradhan, C. Sripan, R. Ganesan, Influence of Ge addition on the optical properties of $As_{40}Se_{50}Ge_{10}$ thin film probed by spectroscopy techniques, Phase Trans. 91 (2018) 477–489, http://dx.doi.org/10.1080/01411594.2018.1424337.
[27] G.J. Adriaenssens, Amorphous semiconductors: optical characteristics, in: Encycl. Mater. Sci. Technol., Elsevier, 2001, pp. 283–287, http://dx.doi.org/10.1016/B0-08-043152-6/00060-7.
[28] S.R. Kodigala, Optical Properties of I-III-VI2 Compounds, 2010, pp. 195–317, http://dx.doi.org/10.1016/B978-0-12-373697-0.00005-5.
[29] R. Todorov, E. Černošková, P. Knotek, Z. Černošek, M. Vlasova, Temperature dependence of the optical properties of thin Ge–Se–In films, J. Non. Cryst. Solids 498 (2018) 415–421, http://dx.doi.org/10.1016/j.jnoncrysol.2018.02.038.
[30] Y. Caglar, S. Ilican, M. Caglar, Single-oscillator model and determination of optical constants of spray pyrolyzed amorphous SnO_2 thin films, Eur. Phys. J. B 58 (2007) 251–256, http://dx.doi.org/10.1140/epjb/e2007-00227-y.